



# 1 Introduction

The ever-growing access to high performance computing in scientific communities has enabled development of complex computer models in fields such as nuclear physics, climatology, and engineering that produce massive amounts of data. These models need real-time calibration with quantified uncertainties. Bayesian methodology combined with Gaussian process modeling has been heavily utilized for calibration of computer models due to its natural way to account for various sources of uncertainty; see Higdon et al. (2015), and King et al. (2019) for examples in nuclear physics, Sexton et al. (2012) and Pollard et al. (2016) for examples in climatology, and Lawrence et al. (2010), Plumlee et al. (2016) and Zhang et al. (2019) for applications in engineering, astrophysics, and medicine.

The original framework for Bayesian calibration of computer models was developed by Kennedy and O’Hagan (2001) with extensions provided by Higdon et al. (2005, 2008); Bayarri et al. (2007); Plumlee (2017, 2019), and Gu and Wang (2018), to name a few. Despite its popularity, however, Bayesian calibration becomes infeasible in big-data scenarios with complex and many-parameter models because it relies on Markov chain Monte Carlo (MCMC) algorithms to approximate posterior densities.

This text presents a scalable and statistically principled approach to Bayesian calibration of computer models. We offer an alternative approximation to posterior densities using variational Bayesian inference (VBI), which originated as a machine learning algorithm that approximates a target density through optimization. Statisticians and computer scientists (starting with Peterson and Anderson (1987); Jordan et al. (1999)) have been widely using variational techniques because they tend to be faster and easier to scale to massive datasets. Moreover, the recently published frequentist consistency of variational Bayes by Wang and Blei (2018) established VBI as a theoretically valid procedure. The scalability of VBI in modern applications hinges on efficiency of stochastic optimization in scenarios with independent data points. This efficiency, however, diminishes in the case of Bayesian calibration of computer models due to dependence structure in data (Robbins and Monro, 1951; Hoffman et al., 2013). To maintain the speed and scalability of VBI, we adopt a pairwise decomposition of data likelihood using vine copulas that separate the information

on dependence structure in data from their marginal distributions (Cooke and Kurowicka, 2006). Our specific contributions are as follows:

1. We propose a novel version of the black-box variational inference (Ranganath et al., 2014) for Bayesian calibration of computer models that preserves the efficiency of stochastic optimization in scenario with dependent data. Python code with our algorithm is available at [https://github.com/kejzlarv/VBI\\_Calibration](https://github.com/kejzlarv/VBI_Calibration).
2. We implement Rao-Blackwellization, control variates, and importance sampling to reduce the variance of noisy gradient estimates involved in our algorithm.
3. We provide both theoretical and empirical evidence for scalability of our methodology and establish its superiority over the Metropolis-Hastings algorithm and the No-U-Turn sampler both in terms of time efficiency and memory requirements.
4. Finally, we demonstrate the opportunities in uncertainty quantification given by the proposed algorithm on a real-world example in the field of nuclear physics.

## 1.1 Outline of this paper

In Section 2, we describe the framework for Bayesian calibration of computer models and give a general overview of VBI. In Section 3, we derive our proposed VBI approach to perform inexpensive and scalable calibration. We establish statistical validity of the method and provide theoretical justification for its scalability. Subsequently, in Section 4, we discuss the implementation details with focus on strategies to reduce the variance of the gradient estimators that are at the center of stochastic optimization for VBI. Section 5 presents a simulation study comparing our approach with the state-of-the-art methods to approximate posterior distribution and illustrates our method on a real-data application.

## 2 Background and Theoretical Framework

Formally, let us consider a computer model  $f(x, \theta)$  relying on a parameter vector  $\theta$  and a vector of inputs  $x$ . Let  $(x_i, y_i)_{i=1}^{m_1}$  be a set of experimental measurements and inputs

of a physical process  $\zeta(x)$ . Model calibration corresponds to determining the unknown and hypothetical *true* value of the parameter  $\theta$ , at which the physical process  $\zeta(x)$  would satisfy  $\zeta(x) = f(x, \theta) + \delta(x)$ ;  $\delta(x)$  is the systematic discrepancy of the model whose form is generally unknown. Overall, we can write the complete statistical model as

$$y_i = f(x_i, \theta) + \delta(x_i) + \sigma(x_i)\epsilon_i. \quad (1)$$

The term  $\sigma(x) > 0$  is a scale function to be parametrized and inferred, and  $\epsilon_i$  are independent random variables representing measurement errors, which we assume to be standard Gaussian. For computationally expensive models, the evaluations of  $f(x, \theta)$  cannot be reasonably performed at calibration runtime: they need to be done beforehand, typically on a grid or otherwise space-filling design. Common practice is to emulate the computer model by a Gaussian process  $\mathcal{GP}(m_f(x, \theta), k_f((x, \theta), (x', \theta')))$  with mean function  $m_f$  and covariance function  $k_f$ . In this setup, the data also include a set of model runs  $z = (z_1, \dots, z_{m_2})$  at predetermined points  $\{(\tilde{x}_1, \tilde{\theta}_1), \dots, (\tilde{x}_{m_2}, \tilde{\theta}_{m_2})\}$ . The discrepancy function  $\delta(x)$ , while intrinsically deterministic, is also modeled by a Gaussian process. Under this framework, the complete dataset  $\mathbf{d} = (d_1, \dots, d_n) := (y, z)$  follows

$$\mathbf{d}|\phi \sim N(M(\phi), K(\phi)), \quad (2)$$

where  $M(\phi)$  and  $K(\phi)$  are the mean and covariance of a multivariate normal distribution. The latent vector  $\phi$  consists of the calibration parameters  $\theta$  and hyperparameters corresponding to the  $\mathcal{GP}$ 's parametrization. The term ‘‘calibration’’ in the Bayesian paradigm includes both parameter estimation and a full evaluation of uncertainty for every parameter under a prior uncertainty expressed by  $p(\phi)$ . We are therefore interested in deriving the posterior distribution  $p(\phi|\mathbf{d})$ . *This becomes quickly infeasible with increasing size of datasets, number of parameters, and model complexity.* Traditional MCMC methods that approximate  $p(\phi|\mathbf{d})$ —such as the Metropolis-Hastings (MH) algorithm (Chib and Greenberg, 1995) or more advanced ones including Hamiltonian Monte Carlo or the No-U-Turn Sampler (NUTS) (Homan and Gelman, 2014)—typically fail because of the computational costs as-

sociated with the evaluation of  $p(\mathbf{d}|\phi)$ . The conventional approaches to scalable Bayesian inference are in general not applicable here because of the highly correlated structure of  $K(\phi)$  or the nature of calibration itself. Indeed, parallelization of MCMC (Neiswanger et al., 2014) works in the case of independent  $\mathbf{d}$ , and Gaussian process approximation methods are developed in the context of regression problems (Quiñonero-Candela and Rasmussen, 2005; Titsias, 2009). We emphasize that our context is much more complex and that our approach is not developing parallel computing, but rather exploiting probabilistic theory of approximation to reduce the computational cost.

## 2.1 Variational Bayes Inference (VBI)

VBI is an optimization based method that approximates  $p(\phi|\mathbf{d})$  by a family of distributions  $q(\phi|\lambda)$  over latent variables with its own variational parameter  $\lambda$ . Many commonly used families exist with the simplest mean-field family assuming independence of all the components in  $\phi$ ; see Hoffman and Blei (2015); Tran et al. (2015); Ranganath et al. (2016) for more examples. The approximate distribution  $q^*$  is chosen to satisfy

$$q^* = \underset{q(\phi|\lambda)}{\operatorname{argmin}} KL(q(\phi|\lambda)||p(\phi|\mathbf{d})). \quad (3)$$

Here,  $KL$  denotes the Kullback-Leibler divergence of  $q(\phi|\lambda)$  from  $p(\phi|\mathbf{d})$ . Finding  $q^*$  is done in practice by maximizing the *evidence lower bound (ELBO)*

$$\mathcal{L}(\lambda) = E_q \left[ \log p(\mathbf{d}|\phi) \right] - KL(q(\phi|\lambda)||p(\phi)), \quad (4)$$

which is a sum of the expected data log-likelihood  $\log p(\mathbf{d}|\phi)$  and the  $KL$  divergence between the combined prior distribution  $p(\phi)$  of calibration parameters and  $\mathcal{GP}$  hyperparameters and the variational distribution  $q(\phi|\lambda)$ . Minimizing the ELBO is equivalent to minimizing the original objective function. Note that we set  $\mathcal{L}(\lambda) := \mathcal{L}(q(\phi|\lambda))$  for the ease of notation. The ELBO is typically optimized via coordinate- or gradient-ascent methods. These techniques are inefficient for large datasets, because we must optimize the variational parameters globally for the whole dataset. Instead, it has become common practice to use a

stochastic gradient ascent (SGA) algorithm, which Hoffman et al. (2013) named “stochastic variational inference” (SVI). Similarly to traditional gradient ascent, SGA updates  $\lambda$  at the  $t^{\text{th}}$  iteration with  $\lambda_{t+1} \leftarrow \lambda_t + \rho_t \tilde{l}(\lambda_t)$ . Here,  $\tilde{l}(\lambda)$  is a realization of the random variable  $\tilde{\mathcal{L}}(\lambda)$ , so that  $E(\tilde{\mathcal{L}}(\lambda)) = \nabla_{\lambda} \mathcal{L}(\lambda)$ , and Ranganath et al. (2014) shows that the gradient of ELBO with respect to the variational parameter  $\lambda$  can be written as

$$\nabla_{\lambda} \mathcal{L}(\lambda) = E_q \left[ \nabla_{\lambda} \log q(\phi|\lambda) (\log p(\mathbf{d}|\phi) - \log \frac{q(\phi|\lambda)}{p(\phi)}) \right], \quad (5)$$

where  $\nabla_{\lambda} \log q(\phi|\lambda)$  is the gradient of the variational log-likelihood with respect to  $\lambda$ . SGA converges to a local maximum of  $\mathcal{L}(\lambda)$  (global for  $\mathcal{L}(\lambda)$  concave (Bottou et al., 1997)) when the learning rate  $\rho_t$  follows the Robbins-Monro conditions (Robbins and Monro, 1951)

$$\sum_{t=1}^{\infty} \rho_t = \infty, \quad \sum_{t=1}^{\infty} \rho_t^2 < \infty. \quad (6)$$

The bottleneck in the computation of  $\nabla_{\lambda} \mathcal{L}(\lambda)$  is the evaluation of the log-likelihood  $\log p(\mathbf{d}|\phi)$ , which makes traditional gradient methods as hard to scale as MCMC methods. SGA algorithms address this challenge. Indeed, if we consider  $d_i \sim p(d_i|\phi)$  independent observations, then we can define a noisy estimate of the gradient  $\nabla_{\lambda} \mathcal{L}(\lambda)$  as

$$\tilde{\mathcal{L}}(\lambda) := n E_q \left[ \nabla_{\lambda} \log q(\phi|\lambda) (\log p(d_I|\phi)) \right] - E_q \left[ \nabla_{\lambda} \log q(\phi|\lambda) \log \frac{q(\phi|\lambda)}{p(\phi)} \right], \quad (7)$$

where  $I \sim U(1, \dots, n)$  with  $E(\tilde{\mathcal{L}}(\lambda)) = \nabla_{\lambda} \mathcal{L}(\lambda)$ . Each update of  $\lambda$  computes the likelihood only for one observation  $d_i$  at a time and makes the SVI scalable for large datasets. One can easily see that, under the framework for Bayesian calibration,  $E(\tilde{\mathcal{L}}(\lambda)) \neq \nabla_{\lambda} \mathcal{L}(\lambda)$  and that the corresponding **SVI does not scale**.

### 3 Variational Calibration of Computer Models

In this section, we derive the algorithm for scalable variational inference approach to Bayesian computer model calibration. The first step is finding a convenient decomposi-

tion of the likelihood  $p(\mathbf{d}|\phi)$  that allows for an unbiased stochastic estimate of the gradient  $\nabla_{\lambda}\mathcal{L}(\lambda)$  that depends only on a small subset of data. Multivariate copulas, and specifically their pairwise construction which we shall introduce below, provide such a decomposition. We are not the first ones to use copulas in the context of VBI. For instance, Tran et al. (2015) and Smith et al. (2020) proposed a multivariate copula as a possible variational family. However, we are the first ones using copulas in the context of computer model calibration implementing via VBI.

### 3.1 Multivariate Copulas and Likelihood Decomposition

Fundamentally, a copula separates the information on the dependence structure of  $n > 1$  random variables  $X_1, \dots, X_n$  from their marginal distributions. Let us assume, for simplicity, that the marginal CDFs  $F_1, \dots, F_n$  are continuous and possess inverse functions  $F_1^{-1}, \dots, F_n^{-1}$ . It follows from the probability integral transform that  $U_i := F_i(X_i) \sim U(0, 1)$  and conversely that  $X_i = F_i^{-1}(U_i)$ . With this in mind, we have

$$P(X_1 \leq F_1^{-1}(x_1), \dots, X_n \leq F_n^{-1}(x_n)) = P(U_1 \leq x_1, \dots, U_n \leq x_n) := C(x_1, \dots, x_n).$$

The function  $C$  is a distribution with support on  $[0, 1]^n$ , uniform marginals, and is called a copula. A one-to-one correspondence exists between copula  $C$  and the distribution of  $\mathbf{X} = (X_1, \dots, X_n)^T$ , as stated in the following theorem due to Sklar (1959). To keep the notation consistency and readability, we re-state the theorem here.

**Theorem 1 (Sklar (1959))** *Given random variables  $X_1, \dots, X_n$  with continuous marginals  $F_1, \dots, F_n$  and joint distribution functions  $F$ , there exists a unique copula  $C$  such that for all  $\mathbf{x} = (x_1, \dots, x_n)^T \in \mathbb{R}^n$ :  $F(x_1, \dots, x_n) = C(F_1(x_1), \dots, F_n(x_n))$ . Conversely, given  $F_1, \dots, F_n$  and copula  $C$ ,  $F$  defined through  $C(F_1(x_1), \dots, F_n(x_n))$  is an  $n$ -variate distribution functions with marginals  $F_1, \dots, F_n$ .*

Consequently, one can write the joint pdf  $f$  of  $\mathbf{X} = (X_1, \dots, X_n)^T$  as

$$f(x_1, \dots, x_n) = c(F_1(x_1), \dots, F_n(x_n)) \prod_{i=1}^n f_i(x_i), \quad (8)$$

where  $c$  represents the copula density and  $f_i$  is the marginal of  $X_i$ .

The key reason for considering copulas is that one can decompose the  $n$ -dimensional copula density  $c$  into a product of bivariate copulas. The starting point for this construction is the recursive decomposition of the density  $f$  into a product of conditional densities

$$f(x_1, \dots, x_n) = \prod_{i=2}^n f(x_i | x_1, \dots, x_{i-1}) f(x_1). \quad (9)$$

For  $n = 2$ , Sklar's theorem implies that  $f(x_1, x_2) = c_{12}(F_1(x_1), F_2(x_2)) f_1(x_1) f_2(x_2)$  and

$$f(x_1 | x_2) = c_{12}(F_1(x_1), F_2(x_2)) f_1(x_1), \quad (10)$$

where  $c_{12} := c_{12}(F_1(x_1), F_2(x_2))$  is a density of  $C(F_1(x_1), F_2(x_2)) = F(x_1, x_2)$ . Using (10) for the decomposition of  $(X_1, X_t)$  given  $X_2, \dots, X_{t-1}$ , we obtain

$$f(x_t | x_1, \dots, x_{t-1}) = \left( \prod_{s=1}^{t-2} c_{s,t;s+1,\dots,t-1} \right) c_{(t-1),t} \cdot f_t(x_t), \quad (11)$$

where  $c_{i,j;i_1,\dots,i_k} := c_{i,j;i_1,\dots,i_k}(F(x_i | x_{i_1}, \dots, x_{i_k}), F(x_j | x_{i_1}, \dots, x_{i_k}))$  and  $F(x_i, x_j | x_{i_1}, \dots, x_{i_k}) := C_{i,j;i_1,\dots,i_k}(F(x_i | x_{i_1}, \dots, x_{i_k}), F(x_j | x_{i_1}, \dots, x_{i_k}))$ .

Using (9) and (11) with the specific index choices  $s = i, t = i + j$ , we have that

$$f(x_1, \dots, x_n) = \left[ \prod_{j=1}^{n-1} \prod_{i=1}^{n-j} c_{i,(i+j);(i+1),\dots,(i+j-1)} \right] \prod_{k=1}^n f_k(x_k). \quad (12)$$

Note that  $c_{i,j;i_1,\dots,i_k}$  are two-dimensional copulas evaluated at CDFs  $F(x_i | x_{i_1}, \dots, x_{i_k})$  and  $F(x_j | x_{i_1}, \dots, x_{i_k})$ . The decomposition above is called a *D-vine distribution*. Similar class of decomposition is possible when one applies (10) on  $(X_{t-1}, X_t)$  given  $X_1, \dots, X_{t-2}$  and sets  $j = t - k, j + i = t$  to get a *canonical vine (C-vine)* (Cooke and Kurowicka, 2006):

$$f(x_1, \dots, x_n) = f_1(x_1) \left[ \prod_{t=2}^n \prod_{k=1}^{t-1} c_{t-k,t;1,\dots,(t-k-1)} \cdot f_t(x_t) \right] = \left[ \prod_{j=1}^{n-1} \prod_{i=1}^{n-j} c_{j,(j+i);1,\dots,(j-1)} \right] \prod_{k=1}^n f_k(x_k).$$

One can imagine that many such decompositions exist. Bedford and Cooke (2002) observed

that these can be represented graphically as a sequence of nested trees with undirected edges, which are referred to as *vine trees* and their decompositions as regular vines.

Here, we focus exclusively on D-vine and C-vine decompositions because they represent the most-studied instances of regular vines and provide especially efficient notation. We note, however, that the following results can be extended to any regular vines.

**Properties of vine copulas (Cooke and Kurowicka, 2006):** The vine copula construction is attractive for two reasons. First, each pair of variables occurs only once as a conditioning set. Second, the bivariate copulas have convenient form in the case of Gaussian likelihood  $f$ . Let  $\mathbf{X} = (X_1, \dots, X_n)^T$  follows a multivariate normal distribution with  $F_j = \Phi, j = 1, \dots, n$ , where  $\Phi$  is the standard normal CDF. The bivariate copula density is

$$c_{i,j;i_1,\dots,i_k}(u_i, u_j) = \frac{1}{\sqrt{1-\theta^2}} \exp\left\{-\frac{\theta^2(w_i^2 + w_j^2) - 2\theta w_i w_j}{2(1-\theta^2)}\right\}. \quad (13)$$

Here,  $u_i = F(x_i|x_{i_1}, \dots, x_{i_k})$ ,  $u_j = F(x_j|x_{i_1}, \dots, x_{i_k})$ ,  $w_i = \Phi^{-1}(u_i)$ ,  $w_j = \Phi^{-1}(u_j)$ , and  $\theta = \rho_{i,j;i_1,\dots,i_k}$  is the partial correlation of variables  $i, j$  given  $i_1, \dots, i_k$ . The D-vine and C-vine decompositions also involve conditional CDFs, for which we need further expressions. Let  $v \in D$  and  $D_{-v} := D \setminus v$  so that  $D$  contains more than one element,  $F(x_j|\mathbf{x}_D)$  is typically computed recursively as  $F(x_j|\mathbf{x}_D) = h(F(x_j|\mathbf{x}_{D_{-v}}), F(x_v|\mathbf{x}_{D_{-v}})|\theta_{jv|D_{-v}})$  and the function  $h$  is for the Gaussian case given by

$$h(u_i, u_j|\rho_{i,j;i_1,\dots,i_k}) = \Phi\left(\frac{\Phi^{-1}(u_i) - \rho_{i,j;i_1,\dots,i_k}\Phi^{-1}(u_j)}{\sqrt{1 - \rho_{i,j;i_1,\dots,i_k}^2}}\right). \quad (14)$$

### 3.2 Scalable Algorithm with Truncated Vine Copulas

We now consider the data likelihood  $p(\mathbf{d}|\phi)$  according to (1) and make use of vines to construct a noisy estimate of the gradient  $\nabla_\lambda \mathcal{L}(\lambda)$ . The log-likelihood  $\log p(\mathbf{d}|\phi)$  can be rewritten according to the D-vine decomposition as

$$\log p(\mathbf{d}|\phi) = \sum_{j=1}^{n-1} \sum_{i=1}^{n-j} p_{i,i+j}^D(\phi), \quad (15)$$

where  $p_{i,i+j}^D(\phi) = \log c_{i,(i+j):(i+1),\dots,(i+j-1)} + \frac{1}{n-1}(\log p_i(d_i|\phi) + \log p_{i+j}(d_{i+j}|\phi))$ . This can be conveniently used in the expression of the ELBO gradient. For D-vine, we have that

$$\nabla_\lambda \mathcal{L}(\lambda) = \sum_{j=1}^{n-1} \sum_{i=1}^{n-j} E_q \left[ \nabla_\lambda \log q(\phi|\lambda)(p_{i,i+j}^D(\phi)) \right] - E_q \left[ \nabla_\lambda \log q(\phi|\lambda) \log \frac{q(\phi|\lambda)}{p(\phi)} \right]. \quad (16)$$

Additionally, if we consider the bijection

$$I_D : \left\{1, \dots, \frac{n(n-1)}{2}\right\} \rightarrow \{(i, i+j) : i \in \{1, \dots, n-j\} \text{ for } j \in \{1, \dots, n-1\}\} \quad (17)$$

and the random variable  $K \sim U(1, \dots, \frac{n(n-1)}{2})$ , we define an estimate of the gradient as

$$\tilde{\mathcal{L}}_D(\lambda) := \frac{n(n-1)}{2} E_q \left[ \nabla_\lambda \log q(\phi|\lambda)(p_{I_D(K)}^D(\phi)) \right] - E_q \left[ \nabla_\lambda \log q(\phi|\lambda) \log \frac{q(\phi|\lambda)}{p(\phi)} \right]. \quad (18)$$

This is unbiased (i.e.,  $E(\tilde{\mathcal{L}}_D(\lambda)) = \nabla_\lambda \mathcal{L}(\lambda)$ ) as desired. Similarly, we can derive a noisy estimate  $\tilde{\mathcal{L}}_C(\lambda)$  of the gradient using C-vine. We leave the details to the Appendix A. As in the case of SVI for independent data, these noisy estimates allow to update the variational parameter  $\lambda$  without the need to evaluate the whole likelihood  $p(\mathbf{d}|\phi)$ . We need to consider only the data consisting of a copula's conditioning and conditioned sets. Unfortunately, both  $\tilde{\mathcal{L}}_D(\lambda)$  and  $\tilde{\mathcal{L}}_C(\lambda)$  can be relatively costly to compute for large datasets because of the recursive nature of calculations involved in the copula densities' evaluation. According to Brechmann et al. (2012); Brechmann and Joe (2015), and Dissmann et al. (2013), the most important and strongest dependencies among variables can typically be captured best by the pair copulas of the first trees. This notion motivates the use of *truncated vine copulas*, where the copulas associated with higher-order trees are set to independence copulas. From the definition of a regular vine, one can show that a joint density  $f$  can be decomposed as

$$f(x_1, \dots, x_n) = \left[ \prod_{j=1}^{n-1} \prod_{e \in E_j} c_{j(e),k(e);D(e)} \right] \prod_{k=1}^n f_k(x_k),$$

where  $e = j(e), k(e); D(e) \in E_j$  is an edge in the  $j^{\text{th}}$  tree of the vine specification. We define the truncated regular vine copula as follows.

**Definition 1 (Brechmann et al. (2012))** Let  $\mathbf{U} = \{U_1, \dots, U_n\}$  be a random vector with uniform marginals, and let  $l \in \{1, \dots, n-1\}$  be the truncation level. Let  $\Pi$  denote the bivariate independence copula. Then  $\mathbf{U}$  is said to be distributed according to an  $n$ -dimensional  $l$ -truncated  $R$ -vine copula if  $C$  is an  $n$ -dimensional  $R$ -vine copula with

$$C_{j(e),k(e);D(e)} = \Pi \quad \forall e \in E_i \quad i = l+1, \dots, n-1.$$

For the case of an **l-truncated D-vine**, we have

$$f(x_1, \dots, x_n) = \left[ \prod_{j=1}^l \prod_{i=1}^{n-j} c_{i,(i+j);(i+1),\dots,(i+j-1)} \right] \prod_{k=1}^n f_k(x_k). \quad (19)$$

If the copula of  $p(\mathbf{d}|\phi)$  is distributed according to an  $l$ -truncated D-vine, we can rewrite

$$\log p(\mathbf{d}|\phi) = \sum_{j=1}^l \sum_{i=1}^{n-j} p_{i,i+j}^{D_l}(\phi), \quad (20)$$

where  $p_{i,i+j}^{D_l}(\phi) = \log c_{i,(i+j);(i+1),\dots,(i+j-1)} + \frac{1}{a_i} \log p_i(d_i|\phi) + \frac{1}{b_{i+j}} \log p_{i+j}(d_{i+j}|\phi)$ , and

$$a_i = 2l - \left[ (l+1-i)\mathbb{1}_{i \leq l} + (l-n+i)\mathbb{1}_{i > n-l} \right], \quad (21)$$

$$b_{i+j} = 2l - \left[ (l+1-j-i)\mathbb{1}_{i+j \leq l} + (l-n+j+i)\mathbb{1}_{i+j > n-l} \right]. \quad (22)$$

The main idea for the scalable variational calibration (VC) of computer models is replacing the full log-likelihood  $\log(\mathbf{d}|\phi)$  in the definition of ELBO with the likelihood based on a truncated vine copula. This yields the *l-truncated ELBO* for the  $l$ -truncated D-vine:

$$\mathcal{L}_{D_l}(\lambda) = E_q \left[ \sum_{j=1}^l \sum_{i=1}^{n-j} p_{i,i+j}^{D_l}(\phi) \right] - KL(q(\phi|\lambda) || p(\phi)). \quad (23)$$

Given the bijection

$$I_{D_l} : \left\{ 1, \dots, \frac{l(2n-(l+1))}{2} \right\} \rightarrow \left\{ (i, i+j) : i \in \{1, \dots, n-j\} \text{ for } j \in \{1, \dots, l\} \right\} \quad (24)$$

and  $K \sim U(1, \dots, \frac{l(2n-(l+1))}{2})$ , we can get an estimate of the gradient  $\nabla_\lambda \mathcal{L}_{D_l}(\lambda)$  from

$$\tilde{\mathcal{L}}_{D_l}(\lambda) := \frac{l(2n-(l+1))}{2} E_q \left[ \nabla_\lambda \log q(\phi|\lambda)(p_{I_{D_l}(K)}^{D_l}(\phi)) \right] - E_q \left[ \nabla_\lambda \log q(\phi|\lambda) \log \frac{q(\phi|\lambda)}{p(\phi)} \right],$$

which is unbiased since  $E(\tilde{\mathcal{L}}_{D_l}(\lambda)) = \nabla_\lambda \mathcal{L}_{D_l}(\lambda)$ . We can analogously derive an unbiased estimate  $\tilde{\mathcal{L}}_{C_l}(\lambda)$  of the gradient using C-vine (see Appendix A). Considering the  $l$ -truncated ELBO (23), our proposed algorithm for the VC of computer models with truncated vine copulas is stated in the Algorithm 1. Note that  $\tilde{\mathcal{L}}_{D_l}(\lambda)$  does not have closed form expression in general due to expectations involved in the computation. Therefore, we resort to a Monte Carlo (MC) approximation of  $\tilde{\mathcal{L}}_{D_l}(\lambda)$  using samples from the variational distribution.

---

**Algorithm 1** Variational Calibration with Truncated Vine Copulas (D-vine version)

---

**Require:** Data  $\mathbf{d}$ , mean and covariance functions for  $\mathcal{GP}$  models in Kennedy-O’Hagan framework, variational family  $q(\phi|\lambda)$ , **truncation level  $l$**

- 1:  $\lambda \leftarrow$  random initial value
  - 2:  $t \leftarrow 1$
  - 3: **repeat**
  - 4:     **for**  $s = 1$  to  $S$  **do** ▷ Random sample  $q$
  - 5:          $\phi[s] \sim q(\phi|\lambda)$
  - 6:     **end for**
  - 7:      $K \leftarrow U(1, \dots, \frac{l(2n-(l+1))}{2})$
  - 8:      $\rho \leftarrow t^{\text{th}}$  value of a Robbins-Monro sequence
  - 9:      $\lambda \leftarrow \lambda + \rho \frac{1}{S} \sum_{s=1}^S \left[ \frac{l(2n-(l+1))}{2} \nabla_\lambda \log q(\phi[s]|\lambda)(p_{I_{D_l}(K)}^{D_l}(\phi[s]) - \frac{2}{l(2n-(l+1))} \log \frac{q(\phi[s]|\lambda)}{p(\phi[s])}) \right]$
  - 10:     $t \leftarrow t + 1$
  - 11: **until** change of  $\lambda$  is less than  $\epsilon$
- 

**Scalability Discussion:** The complexity of bivariate copula evaluation depends on the size of conditioning dataset due to the recursive nature of the calculations (Cooke and Kurowicka, 2006). From the vine tree construction, the cardinality of the conditioning set for D-vine and C-vine is in the worst case  $n-2$ . Nevertheless, on average, we can do better. Indeed, let  $X$  be the cardinality of the conditioning set in  $p_{I_D(K)}^D$  (or  $p_{I_C(K)}^C$ ), then

$$P(X = i) = \frac{n - (i + 1)}{\binom{n}{2}} \quad \text{for } i \in \{0, \dots, n - 2\} \quad (25)$$

and  $E(X) = \frac{n-2}{3}$ . The cardinality of conditioning set is on average roughly  $n/3$ . On the other hand, the cardinality of conditioning set is for the case of Algorithm 1 at most  $l - 1$ . Now, let  $X$  be the cardinality of the conditioning set in the updating step of the variational parameter  $\lambda$  in the Algorithm 1, then

$$P(X = i) = \frac{n - (i + 1)}{\frac{l(2n - (l + 1))}{2}} \quad \text{for} \quad i \in \{0, \dots, l - 1\}, \quad (26)$$

and  $E(X) = [(l - 1)(3n - 2l - 2)]/[3(2n - l - 1)]$ .  $E(X) \approx 2$  for  $n = 10^5$  and truncation level  $l = 5$ , which is a significant improvement to the average case  $p_{I_D(K)}^D$  and  $p_{I_C(K)}^C$  ( $\approx 33333$  for  $n = 10^5$ ). This provides a heuristic yet convincing argument for the scalability.

## 4 Implementation Details

### 4.1 Selection of Truncation Level

Selection of the truncation level  $l$  is an important element of effective approximation of the posterior distribution  $p(\phi|\mathbf{d})$  under the Algorithm 1. Dissmann et al. (2013) propose a sequential approach for selection of  $l$  in the case of vine estimation. One sequentially fits models with an increasing truncation level until the quality of fit stays stable or computational resources are depleted. We adopt similar idea for the case of VC of computer models with vine copulas. Let  $\lambda(l)$  represents the value of variational parameter estimated with the Algorithm 1 for a fixed truncation level  $l$ . One can then sequentially increase  $l$  until  $\Delta(\lambda(l + 1), \lambda(l)) < \epsilon$  for some distance metric  $\Delta$  and a desired tolerance  $\epsilon$ .

### 4.2 Variance Reduction of Monte Carlo Approximations

The computational convenience of simple MC approximations of the gradient estimators based on  $l$ -truncated D-vine and C-vine copulas,  $\tilde{\mathcal{L}}_{D_l}(\lambda)$  and  $\tilde{\mathcal{L}}_{C_l}(\lambda)$  (see Section 3.2) is typically accompanied by their large variance. The consequence in practice is a need for small step size  $\rho_t$  in the SGA portion of the Algorithm 1 which results in slower convergence. In order to reduce the variance of MC approximations, we adopt the same approach as Ruiz

et al. (2016) and use Rao-Blackwellization (Casella and Robert, 1996) in combination with control variates (CV) (Ross, 2006) and importance sampling. The remainder of this section focuses on the case of D-vine decomposition, see Appendix A for derivations for C-vines.

### 4.2.1 Rao-Blackwellization

The idea here is to replace the noisy estimate of gradient with its conditional expectation with respect to a subset of  $\phi$ . For simplicity, let us consider a situation with  $\phi = (\phi_1, \phi_2) \in \mathbb{R}^2$  and variational family  $q(\phi|\lambda)$  that factorizes into  $q(\phi_1|\lambda_1)q(\phi_2|\lambda_2)$ . Additionally, let  $\hat{\mathcal{L}}_\lambda(\phi_1, \phi_2)$  be the MC approximation of the gradient  $\nabla_\lambda \mathcal{L}(\lambda)$ . Now, the conditional expectation  $E[\hat{\mathcal{L}}_\lambda(\phi_1, \phi_2)|\phi_1]$  is also an unbiased estimate of  $\nabla_\lambda \mathcal{L}(\lambda)$  since  $E_q(E[\hat{\mathcal{L}}_\lambda(\phi_1, \phi_2)|\phi_1]) = E_q(\hat{\mathcal{L}}_\lambda(\phi_1, \phi_2))$  and

$$\text{Var}_q(E[\hat{\mathcal{L}}_\lambda(\phi_1, \phi_2)|\phi_1]) = \text{Var}_q(\hat{\mathcal{L}}_\lambda(\phi_1, \phi_2)) - E[(\hat{\mathcal{L}}_\lambda(\phi_1, \phi_2) - E[\hat{\mathcal{L}}_\lambda(\phi_1, \phi_2)|\phi_1])^2]$$

shows that  $\text{Var}_q(E[\hat{\mathcal{L}}_\lambda(\phi_1, \phi_2)|\phi_1]) \leq \text{Var}_q(\hat{\mathcal{L}}_\lambda(\phi_1, \phi_2))$ . The factorization of the variational family also makes the conditional expectation straightforward to compute as

$$E[\hat{\mathcal{L}}_\lambda(\phi_1, \phi_2)|\phi_1] = \int_\phi E[\hat{\mathcal{L}}_\lambda(\phi_1, \phi_2)] \frac{q(\phi_1|\lambda_1)q(\phi_2|\lambda_2)}{q(\phi_1|\lambda_1)} = E_{q(\phi_2|\lambda_2)}(\hat{\mathcal{L}}_\lambda(\phi_1, \phi_2)),$$

i.e., we just need to integrate out some variables. Let us consider the MC approximation of the gradient estimator  $\tilde{\mathcal{L}}_{D_l}(\lambda)$ . The  $j^{\text{th}}$  entry of the Rao-Blackwellized estimator is

$$\frac{1}{S} \sum_{s=1}^S \left[ \frac{l(2n - (l + 1))}{2} \nabla_{\lambda_j} \log q(\phi_j[s]|\lambda_j) (\tilde{p}_{(j)}(\phi[s]) - \frac{2}{l(2n - (l + 1))} \log \frac{q(\phi_j[s]|\lambda_j)}{p(\phi_j[s])}) \right],$$

where  $\tilde{p}_{(j)}(\phi)$  are the components of  $p_{I_{D_l}(K)}^{D_l}(\phi)$  that include  $\phi_j$ .

### 4.2.2 Control Variates

To further reduce the variance of the MC approximations we will replace the Rao-Blackwellized estimate above with a function that has equivalent expectation but again smaller variance. For illustration, let us first consider a target function  $\xi(\phi)$  whose variance we want to

reduce, and a function  $\psi(\phi)$  with finite expectation. Define

$$\hat{\xi}(\phi) = \xi(\phi) - a(\psi(\phi) - E_q(\psi(\phi))), \quad (27)$$

where  $a$  is a scalar and  $E_q(\hat{\xi}(\phi)) = E_g(\xi(\phi))$ . The variance of  $\hat{\xi}(\phi)$  is

$$\text{Var}_q(\hat{\xi}(\phi)) = \text{Var}_q(\xi(\phi)) + a^2 \text{Var}_q(\psi(\phi)) - 2a \text{Cov}_q(\xi(\phi), \psi(\phi)). \quad (28)$$

This shows that a good choice for function  $\psi(\phi)$  is one that has high covariance with  $\xi(\phi)$ . Moreover, the value of  $a$  that minimizes (28) is

$$a^* = \frac{\text{Cov}_q(\xi(\phi), \psi(\phi))}{\text{Var}_q(\psi(\phi))}. \quad (29)$$

Let us place CV back into the context of calibration. Meeting the above described criteria, Ranganath et al. (2014) propose  $\psi(\phi)$  to be  $\nabla_\lambda \log q(\phi|\lambda)$ , because it depends only on the variational distribution and has expectation zero. We can now set the target function  $\xi(\phi)$  to be  $\frac{l(2n-(l+1))}{2} \nabla_{\lambda_j} \log q(\phi_j|\lambda_j)(\tilde{p}_{(j)}(\phi) - \frac{2}{l(2n-(l+1))} \log \frac{q(\phi_j|\lambda_j)}{p(\phi_j)})$ , which gives the following  $j^{\text{th}}$  entry of the MC approximation of the gradient estimator  $\tilde{\mathcal{L}}_{D_l}(\lambda)$  with CV

$$\tilde{\mathcal{L}}_{D_l}^{CV(j)}(\lambda) = \frac{1}{S} \sum_{s=1}^S \left[ \frac{l(2n-(l+1))}{2} \nabla_{\lambda_j} \log q(\phi_j[s]|\lambda_j)(\tilde{p}_{(j)}(\phi[s]) - \frac{2(\log \frac{q(\phi_j[s]|\lambda_j)}{p(\phi_j[s])} + \hat{a}_j^D)}{l(2n-(l+1))}) \right],$$

where  $\hat{a}_j^D$  is the estimate of  $a^*$  based on additional independent draws from the variational approximation (otherwise the estimator would be biased).

### 4.2.3 Importance sampling

Here, we outline the last variance reduction technique that makes use of importance sampling. We refer to Ruiz et al. (2016) for full description of the method and illustration of its efficiency in VI framework. Fundamentally, instead of taking samples from the variational family  $q(\phi|\lambda)$  to carry out the MC approximation of the ELBO gradient, we will take samples from an overdispersed distribution  $r(\phi|\lambda, \tau)$  in the same family that depends

on an additional dispersion parameter  $\tau > 1$ . Namely, we can write the estimate  $\tilde{\mathcal{L}}_{D_l}(\lambda)$  as

$$E_{r(\phi|\lambda, \tau)} \left[ \frac{l(2n - (l + 1))}{2} \nabla_{\lambda} \log q(\phi|\lambda) (p_{I_{D_l}(K)}^{D_l}(\phi) - \frac{2}{l(2n - (l + 1))} \log \frac{q(\phi|\lambda)}{p(\phi)}) w(\phi) \right],$$

where  $w(\phi) = q(\phi|\lambda)/r(\phi|\lambda, \tau)$  is the importance weight which guarantees the estimator to be unbiased. Combining the ideas of Rao-Blackwellization, CV, and importance sampling, we have the following  $j^{\text{th}}$  entry of the MC approximation of the gradient estimator  $\tilde{\mathcal{L}}_{D_l}(\lambda)$

$$\tilde{\mathcal{L}}_{D_l}^{OCV(j)}(\lambda) = \sum_{s=1}^S \left[ \frac{l(2n - (l + 1))}{2S} \nabla_{\lambda_j} \log q(\phi_j[s]|\lambda_j) (\tilde{p}_{(j)}(\phi[s]) - \frac{2(\log \frac{q(\phi_j[s]|\lambda_j)}{p(\phi_j[s])} + \tilde{a}_j^D)}{l(2n - (l + 1))}) w(\phi_j[s]) \right],$$

where  $\phi[s] \sim r(\phi|\lambda, \tau)$  and

$$\tilde{a}_j^D = \frac{\widehat{Cov}_r \left( \frac{l(2n - (l + 1))}{2} \nabla_{\lambda_j} \log q(\phi_j|\lambda_j) (\tilde{p}_{(j)}(\phi) - \frac{2 \log \frac{q(\phi_j|\lambda_j)}{p(\phi_j)}}{l(2n - (l + 1))}) w(\phi_j), \nabla_{\lambda_j} \log q(\phi_j|\lambda_j) w(\phi_j) \right)}{\widehat{Var}_r (\nabla_{\lambda_j} \log q(\phi_j|\lambda_j) w(\phi_j))}.$$

The extension of the Algorithm 1 with the variance reductions of the MC approximations due to Rao-Blackwellization, CV, and importance sampling is summarized in the Algorithm 2.

---

**Algorithm 2** Variational Calibration with Truncated Vine Copulas II (D-vine)

---

**Require:** Data  $\mathbf{d}$ , mean and covariance functions for  $\mathcal{GP}$  models in Kennedy-O'Hagan framework, variational family  $q(\phi|\lambda)$ , dispersion parameter  $\tau$ , **truncation level 1**

- 1:  $\lambda \leftarrow$  random initial value
  - 2:  $t \leftarrow 1$
  - 3: **repeat**
  - 4:   **for**  $s = 1$  to  $S$  **do** ▷ Random sample  $q$
  - 5:      $\phi[s] \sim r(\phi|\lambda, \tau)$
  - 6:   **end for**
  - 7:    $K \leftarrow U(1, \dots, \frac{l(2n - (l + 1))}{2})$
  - 8:    $\rho \leftarrow t^{\text{th}}$  value of a Robbins-Monro sequence
  - 9:    $\lambda \leftarrow \lambda + \rho \sum_{s=1}^S \left[ \frac{l(2n - (l + 1))}{2S} \nabla_{\lambda_j} \log q(\phi_j[s]|\lambda_j) (\tilde{p}_{(j)}(\phi[s]) - \frac{2(\log \frac{q(\phi_j[s]|\lambda_j)}{p(\phi_j[s])} + \tilde{a}_j^D)}{l(2n - (l + 1))}) w(\phi_j[s]) \right]$
  - 10:    $t \leftarrow t + 1$
  - 11: **until** change of  $\lambda$  is less than  $\epsilon$
-

### 4.3 Choice of the learning rate

Even though the SGA is straightforward in its general definition, the choice of learning rate  $\rho_t$  can be challenging in practice. Ideally, one would want the rate to be small in situations where the noisy estimates of the gradient have large variance and vice-versa. The elements of variational parameter  $\lambda$  can also differ in scale, and one needs to set the learning rate so that the SGA can accommodate even the smallest scales. The rapidly increasing usage of machine learning techniques in recent years produced various algorithms for element-wise adaptive-scale learning rates. We use the AdaGrad algorithm (Duchi et al., 2011) which has been considered in similar problems before, e.g., Ranganath et al. (2014), however, there are other popular algorithms such as ADADELTA (Zeiler, 2012) or RMSProp (Tieleman and Hinton, 2012). Let  $g_T$  be the gradient used in the  $T^{\text{th}}$  step of the SGA algorithm, and  $G_t$  be a matrix consisting of the sum of the outer products of these gradients across the first  $t$  iterations, namely

$$G_t = \sum_{T=1}^t g_T g_T^T. \quad (30)$$

AdaGrad defines the element-wise adaptive scale learning rate as  $\rho_t = \eta \cdot \text{diag}(G_t)^{-1/2}$ , where  $\eta$  is the initial learning rate. It is a common practice, however, to add a small constant value to  $\text{diag}(G_t)$  (typically of order  $10^{-6}$ ) to avoid division by zero.

### 4.4 Parametrizations

**Variational Families.** We use a Gaussian distribution for real valued components of  $\phi$  and a gamma distribution for positive variables. Both of these families are parametrized in terms of their mean and standard deviation. Moreover, in order to avoid constrained optimization, we transform all the positive variational parameters  $\lambda$  to  $\tilde{\lambda} = \log(e^\lambda - 1)$  and optimize with respect to  $\tilde{\lambda}$ .

**Overdispersed Families.** Given a fixed dispersion coefficient  $\tau$ , the overdispersed Gaussian distribution with mean  $\mu$  and standard deviation  $\sigma$  is a Gaussian distribution with mean  $\mu$  and standard deviation  $\sigma\sqrt{\tau}$ . The overdispersed gamma distribution with mean  $\mu$

and standard deviation  $\sigma$  is a gamma distribution with mean  $\mu + (\tau - 1)\frac{\sigma^2}{\mu}$  and standard deviation  $\sigma \times \frac{\sqrt{\tau\mu^2 + \tau\sigma^2(\tau-1)}}{\mu}$  (Ruiz et al., 2016).

## 5 Applications

### 5.1 Simulation study

In this section, we study the proposed Algorithm 2 in a simulated scenario, where we first demonstrate the method’s fidelity in approximating the posterior distribution of calibration parameters  $p(\theta|\mathbf{d})$  and substantiate the indispensability of the variance reduction techniques described in Section 4 in order to achieve convergence. Second, we show the scalability of our method in comparison with the popular MH algorithm and the NUTS.

Let us consider a simple scenario following the model (1) with two-dimensional calibration parameter  $\theta = (0.39, 0.60)$  that was obtained as a sample from its prior distribution  $p(\theta)$  and a two-dimensional input variable  $x = (x_1, x_2)$ . We model  $f(x, \theta)$  and  $\delta(x)$  with a Gaussian processes according to the specifications in Table 1.

Table 1: The specification of  $\mathcal{GP}$ s for the simulation study:  $\eta_f = \frac{1}{30}$ ,  $l_x = 1$ ,  $l_\theta = 1$ ,  $\eta_\delta = \frac{1}{30}$ ,  $l_\delta = \frac{1}{2}$ , and  $\beta_\delta = 0.15$

	$\mathcal{GP}$ mean	$\mathcal{GP}$ covariance function
$f$	$\theta_1 \cos(x_1) + \theta_2 \sin(x_2)$	$\eta_f \cdot \exp\left(-\frac{\ x-x'\ ^2}{2l_x^2} - \frac{\ \theta-\theta'\ ^2}{2l_\theta^2}\right)$
$\delta$	$\beta_\delta$	$\eta_\delta \cdot \exp\left(-\frac{\ x-x'\ ^2}{2l_\delta^2}\right)$

We choose the variational family to be the mean-field family with Gaussian distributions for real valued parameters and gamma distributions for positive variables following the parametrization discussed in Section 4.4. The variational parameters are initialized to match the prior distributions, and we use the AdaGrad for stochastic optimization.

#### 5.1.1 Calibration

For the purpose of model calibration, we sampled the data  $\mathbf{d} = (y_1, \dots, y_{m_1}, z_1, \dots, z_{m_2})$  jointly from the prior with experimental noise following  $N(0, \frac{1}{100})$ . The calibration param-

eter values for the model runs  $z$  were selected on a uniform grid over  $[0, 1]^2$  and the inputs  $x$  over  $[0, 3]^2$ . For the first set of experiments, the size of the dataset was  $n = 225$  with  $m_1 = 144$  and  $m_2 = 81$ . We used 50 samples from the variational family to approximate the expectations in the Algorithm 2 and 10 samples to implement the control variates.

Figure 1 demonstrates the quality of the variational approximation (Algorithm 2) in comparison with the MH algorithm and the NUTS. We can see that our method was able to accurately match both MCMC based approximations with minor deviation in  $\theta_1$ . It is important to note, however, that the variance reduction through the combination of Rao-Blackwellization, control variates, and importance sampling was necessary to achieve meaningful convergence.

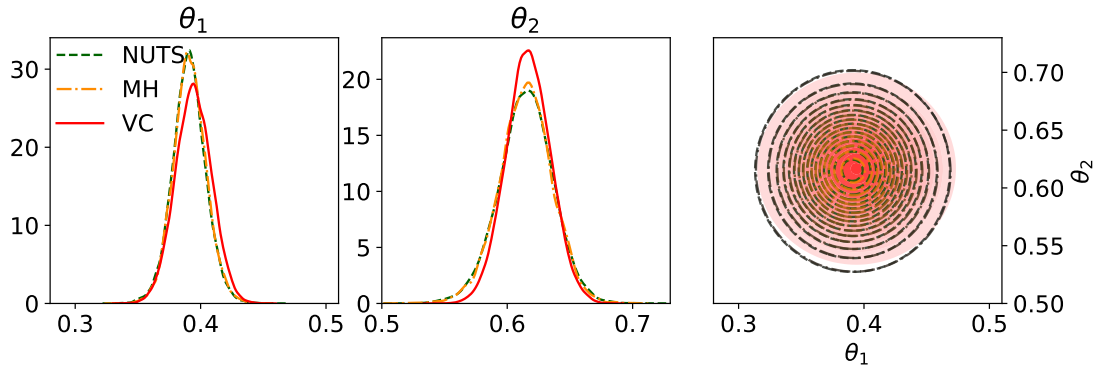


Figure 1: Approximate posterior distributions for the target calibration parameters. The VC (Algorithm 2) was carried out using  $l = 3$  truncated D-vine and compared with the results from the NUTS and the MH algorithm.

In particular, Figure 2 shows the Means Squared Error (MSE) of the posterior predictive means, evaluated on an independently generated set of 50 data points, based on the VC with cumulatively implemented variance reduction techniques. The Algorithm 2 that employs importance sampling clearly outperforms the calibration with only Rao-Blackwellization and the calibration with control variates. In fact, each additional attempt to reduce the variance tends to decrease the MSE by one order of magnitude. There is naturally both time and space (memory) cost associated with each variance reduction technique. Figure 2 shows that control variates and importance sampling practically double the time per iteration of the algorithm. This additional complexity is, however, outweighed by the gain

in the MSE reduction. The increase in memory consumption is less significant and is due to the storage of dispersion coefficients used for importance sampling and samples needed to compute control variates. Note that the memory consumed by the algorithms rises over time, because we chose to store the values of variational parameters during each step; the memory demands can be dramatically reduced if we drop these intermediate results.

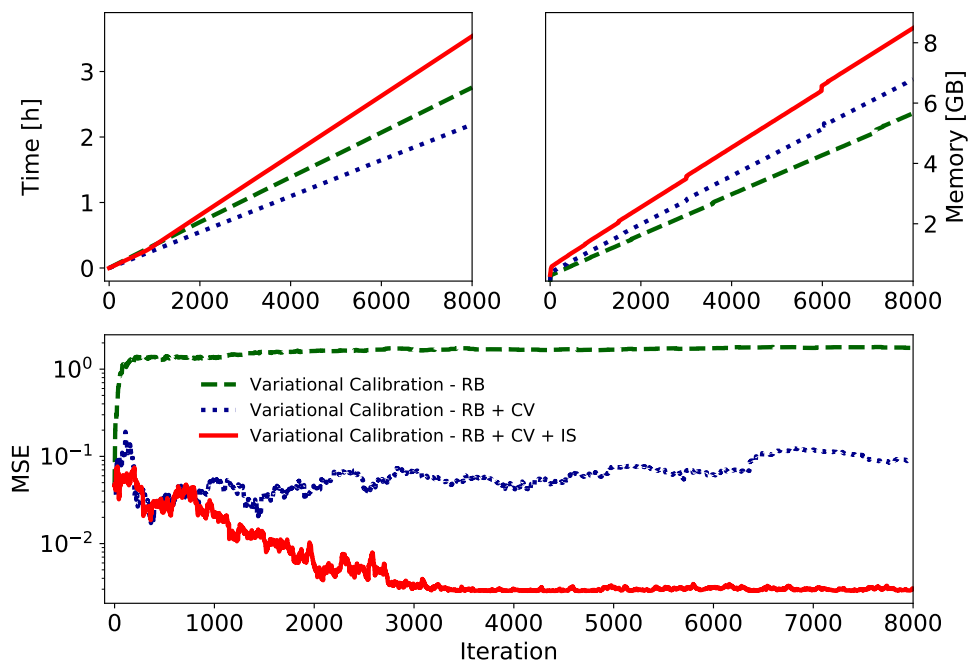


Figure 2: The evolution of MSE of the posterior predictive means based on the VC with cumulatively implemented variance reduction techniques described in Section 4.2. The figure is based on an independently generated set of 50 testing points. Time and memory demands for each of the implementations are plotted as well. The VC (Algorithm 2) was carried out using  $l = 3$  truncated D-vine.

Table 2: Comparison of the MSE for the simple scenario using the MH, the NUTS, and the VC algorithms.

Algorithm	$MSE$
Variational Calibration - RB + CV + IS	$2.9 \times 10^{-3}$
Metropolis-Hastings	$3.0 \times 10^{-3}$
No-U-Turn	$3.0 \times 10^{-3}$

For completeness, in Table 2, we also compare the MSE of MCMC approximations and the VC at the point of convergence of the algorithms. The resulting errors in the predictions were, for all the practical purposes, equivalent.

### 5.1.2 Scalability

We now significantly increase the size of dataset from  $n = 225$  to  $0.5 \times 10^4$  and eventually to  $2 \times 10^4$  with the simulated experimental measurements and the model runs split equally ( $m_1 = m_2$ ). For better numerical stability, we expand the space of the input variables to  $x \in [0, 10]^2$  and select those using the Latin hypercube design (Morris and Mitchell, 1995) which is a space-filling design that has a good coverage of the space with evenly distributed points in each one-dimensional projection. We also enlarge the testing dataset to 200 points. All the remaining simulation parameters are unchanged. The conventional MCMC methods are already impractical for the purpose of Bayesian calibration with these moderately large amounts of data. We were able to obtain only around 600 posterior samples in the case of  $n = 1 \times 10^4$  and about 120 for  $n = 2 \times 10^4$  in 25 hours of sampling using the MH algorithm (significantly less with the NUTS).

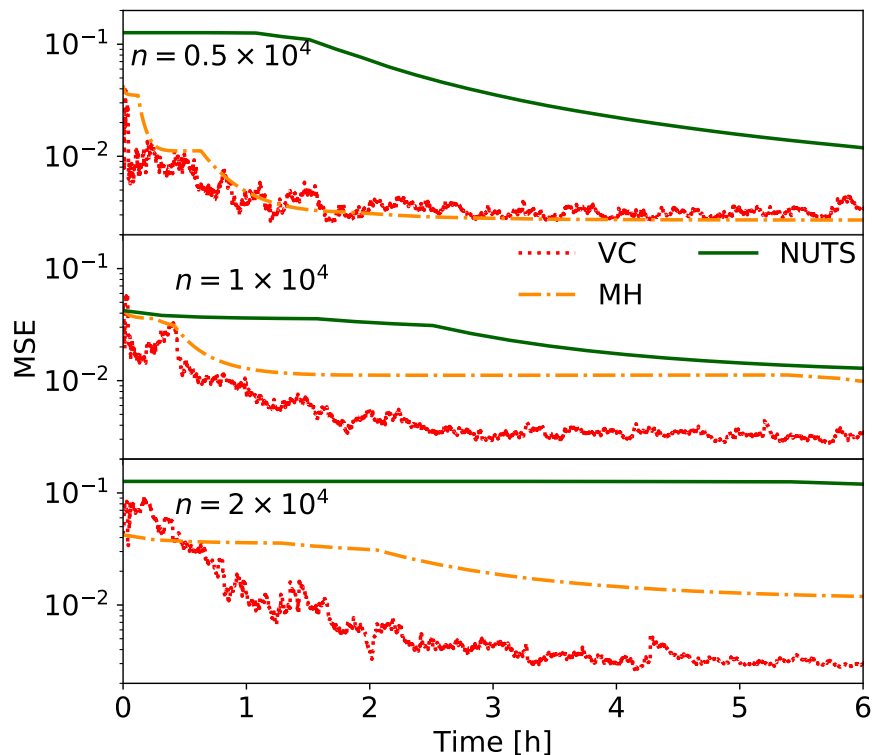


Figure 3: The evolution of the MSE of the posterior predictive means based on the VC (Algorithm 2), the MH algorithm, and the NUTS. The figure is based on an independently generated set of 200 testing points. The VC (Algorithm 2) was carried out using  $l = 5$  truncated D-vine.

Figure 3 demonstrates that the Algorithm 2 (D-vine with truncation  $l = 5$ ) converges to the predictive MSE of about 0.003 under 4h for  $n = 2 \times 10^4$  and 2h for  $n = 0.5 \times 10^4$ . It took similar time for the MH to achieve this MSE value for  $n = 0.5 \times 10^4$  but almost 25h for the NUTS. Once we increased the data size to  $2 \times 10^4$ , neither the NUTS nor the MH were able to achieve similar predictive MSE as the VC within the 25h window allotted for sampling. In fact, they were by an order of magnitude larger. It is important to mention that both MCMC-based algorithms have also substantially larger memory demands than the VC. See Appendix B for more details.

## 5.2 Calibration of Liquid Drop Model

Over the past decade or so, the statistical tools of uncertainty quantification have experienced a robust rump-up in use in the field of nuclear physics. Bayesian calibration has been especially popular because it enhances the understanding of nuclear model’s structure through parameter estimation and potentially advances the quality of nuclear modeling by accounting for systematic errors. In this context, we use our variational Algorithm 2 to calibrate the 4-parameter Liquid Drop Model (LDM) (Myers and Swiatecki, 1966; Kirson, 2008; Benzaid et al., 2020) which is a global (across the whole nuclear chart) model of nuclear binding energies; the minimum energy needed to disassemble the nucleus of an atom into unbound protons and neutrons.

In principle, the LDM treats the nucleus like molecules in a drop of incompressible fluid of very high density. Despite this simplification, the LDM accounts for the spherical shape of most nuclei and makes reasonable estimates of average properties of nuclei. The LDM is formulated through the semi-empirical mass formula as:

$$E_B(N, Z) = a_{\text{vol}}A - a_{\text{surf}}A^{2/3} - a_{\text{sym}}\frac{(N - Z)^2}{A} - a_C\frac{Z(Z - 1)}{A^{1/3}}, \quad (31)$$

where  $Z$  is the proton number,  $N$  is the neutron number, and  $A = Z + N$  is the mass number of an atom. The calibration parameters are  $\theta = (a_{\text{vol}}, a_{\text{surf}}, a_{\text{sym}}, a_C)$  representing the volume, surface, symmetry and Coulomb energy, respectively. These parameters have specific physical meaning, where  $a_{\text{vol}}$  is proportional to the volume of the nucleus for in-

stance. See Krane (1987) for more details. Here we note that this is by no means the first case when Bayesian methodology is applied to study the LDM. In fact, the LDM is a popular model for statistical application (Bertsch et al., 2005; Yuan, 2016; Bertsch and Bingham, 2017) which is why we choose the model to illustrate our methodology as well. The LDM also generally performs better on heavy nuclei as compared to the light nuclei which alludes to the existence of a significant systematic discrepancy between the model and the experimental binding energies (Reinhard et al., 2006; Kejzlar et al., 2020). Namely, we consider the following statistical model

$$y = E_B(N, Z) + \delta(N, Z) + \sigma\epsilon \quad (32)$$

where  $\delta(N, Z)$  represents the unknown systematic discrepancy between the semi-empirical mass formula (31) and the experimental binding energies  $y$ . The parameter  $\sigma$  is the scale of observation error  $\epsilon \sim N(0, 1)$  as usual. The nuclear physics community predominantly (Dobaczewski et al., 2014) considers the least squares (LS) estimator of  $\theta$  defined as

$$\hat{\theta}_{L_2} = \underset{\theta}{\operatorname{argmin}} \sum_{i=1}^n (y_i - E_B(N_i, Z_i))^2 \quad (33)$$

which is also the maximum likelihood estimate of  $\theta$  in the case of  $\delta = 0$ . At this point, it should be clear that this approach neglects some sources of uncertainty (e.g. systematic error) that are accounted for in the Bayesian calibration framework described in Section 2.

To this end, we shall consider a  $\mathcal{GP}$  prior with the mean zero and the squared-exponential covariance function for the systematic discrepancy  $\delta(Z, N)$ . Since the main purpose of the example is to provide a canonical illustration of the methodology in a real data scenario, we also set a  $\mathcal{GP}$  prior for the LDM and treat  $E_B(Z, N)$  as an unknown function. We use 2000 experimental binding energies randomly selected from the AME2003 dataset (Audi et al., 2003) (publicly available at <http://amdc.impcas.ac.cn/web/masstab.html>) for calibration, see Figure 4, and an additional set of  $10^4$  model evaluations. These were generated with the Latin hypercube design for the calibration inputs so that all the reasonable values of  $(a_{\text{vol}}, a_{\text{surf}}, a_{\text{sym}}, a_{\text{C}})$  given by the literature are covered (Weizsäcker, 1935; Bethe and

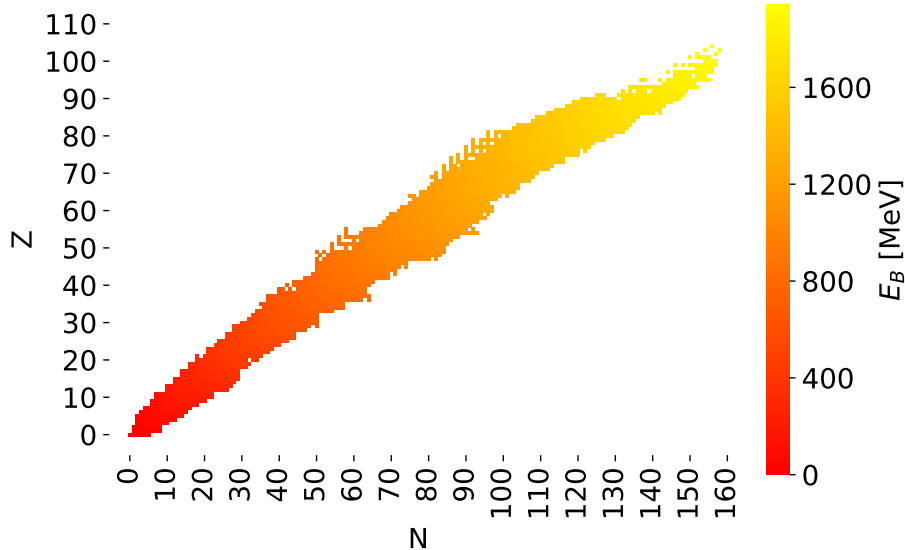


Figure 4: Experimental binding energies of nuclei in AME2003 dataset (2225 observations).

Bacher, 1936; Myers and Swiatecki, 1966; Kirson, 2008; Benzaid et al., 2020). The model inputs  $(Z, N)$  were selected from the set of 2000 experimental binding energies, duplicated five-fold, and randomly permuted among the generated calibration inputs to span only the set of relevant nuclei. This relatively large number of model runs was chosen so that the combined 6 dimensional space of calibration parameters and model inputs is sufficiently covered considering the existence of non-trivial systematic discrepancy. In fact, the uniform experimental design would amount only to 4-5 points per dimension here.

Independent Gaussian distributions centered at the LS estimates  $\hat{\theta}_{L_2}$  (in Table 3) with standard deviations large enough to cover the space of inputs used for generating the model runs were selected to represent the prior knowledge about the calibration parameters. Independent gamma distributions were used as the prior models for the hyperparameters of  $\mathcal{GP}$ 's covariance functions. We choose the variational family to be fully-factorized with the Gaussian distributions for real valued parameters and the gamma distributions for positive variables. The means of variational families were initialized as random samples from their respective prior distributions and the variances were set to match those of the prior distributions. We used the AdaGrad for stochastic optimization. See Appendix C for further discussion on the prior distributions and experimental design.

### 5.2.1 Results

Including the generated model runs, the overall size of training dataset is  $1.2 \times 10^4$  which already makes the MCMC based Bayesian calibration impractical, as illustrated by the simulation study in Section 5.1. We therefore assess the quality of variational approximation against the standard LS estimation with  $\delta = 0$ . In particular, we consider the testing dataset of the remaining 225 experimental binding energies in AME2003 dataset that were excluded from the training data. The predictions  $\hat{y}_{new}$  of these testing binding energies  $y_{new}$  were calculated, under the variational approximation, as the posterior means of  $y_{new}$  conditioned on the  $1.2 \times 10^4$  binding energies from the training data set. The predictions under the LS estimates  $\hat{\theta}_{L_2}$  were given by the semi-empirical mass formula (31).

Table 3 gives the root MSE for both methods under consideration. The VC (Algorithm 2) results are based on a 24h window dedicated for running the algorithm with 50 samples used to approximate the expectations, 10 samples used to implement the control variates, and the truncation level selected to be  $l = 3$ . By using  $\mathcal{GP}$ s to account for the systematic discrepancies of semi-empirical mass formula and the uncertainty of the LDM itself, we were able to significantly reduce the root MSE by approx. 57% compared to the LS benchmark. Table 3 additionally shows the calibration parameter estimates and their standard errors. The estimates under the VC are given by the means of their variational families. Both the methods calibrate the LDM around the same values with notably low standard errors of the LS estimates. This is, however, expected since  $\hat{\theta}_{L_2}$  are ordinary LS estimates that in the presence of heteroscedasticity (see Figure 5) become inefficient and tend to significantly underestimate the true variance (Goldberger, 1966; Johnston, 1976).

Table 3: The root MSE of the VC (Algorithm 2) after 24h dedicated for running the algorithm compared with the root MSE based on the LS estimates. The parameter estimates (and standard errors) are also displayed.

Method	Parameter estimate and standard errors				Testing error
	$a_{vol}$	$a_{surf}$	$a_{sym}$	$a_C$	$\sqrt{MSE}$ (MeV)
LS	15.42 (0.027)	16.91 (0.086)	22.47 (0.070)	0.69 (0.002)	3.54
VC	15.78 (0.198)	15.99 (0.681)	21.94 (0.510)	0.68 (0.018)	1.52

The residual plot in Figure 5 showing the difference between  $y_{new}$  and  $\hat{y}_{new}$  as a function

of the nuclear mass number  $A$  clearly demonstrates a better fit of the testing data with our methodology than is achieved by the simple LS fit. Majority of the residuals appear to be randomly spread around 0 which strongly supports the efficiency of  $\mathcal{GP}$ s in accounting for the systematic discrepancy  $\delta$ .

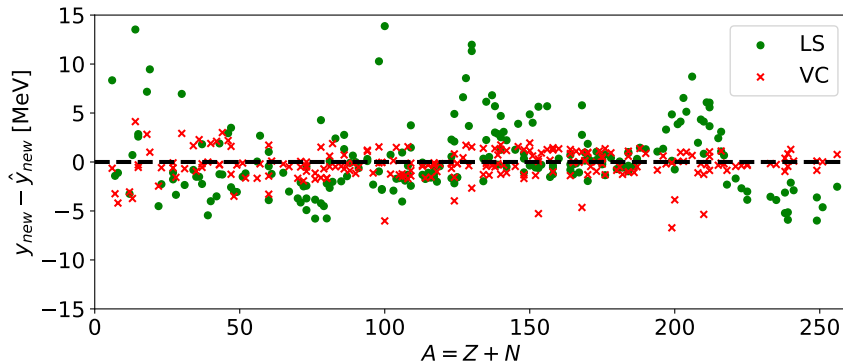


Figure 5: The residual plot for 225 experimental binding energies in the testing dataset.

## 6 Discussion

We developed and studied a VBI based approach to Bayesian calibration of computer models under the celebrated framework of Kennedy and O’Hagan (2001) which has been heavily utilized by practitioners for almost two decades. Our method consists of scalable and statistically principled tools for UQ of computationally complex and many-parameter computer models. We exploit the probabilistic theory of approximation coupled with pairwise construction of multivariate copulas using truncated regular vines to establish these tools. The theoretical justification for scalability was also discussed.

In addition to the general Algorithm given in Section 3.2, we dedicated a significant portion of this text to the description of implementation details that are often neglected in the literature. We discussed the choice of learning rate for stochastic optimization and outlined techniques to reduce the variance of noisy gradient estimates which include the Rao-Blackwellization, control variates, and importance sampling.

In our examples, we first carried out an extensive simulation study that provided empirical evidence for accuracy and scalability of our method in scenarios where traditional

MCMC based approaches become impractical. We established the superiority of the VC over the MH algorithm and the NUTS in terms of time efficiency and memory requirements. We also demonstrated the opportunities given by our method for practitioners on a real data example through calibration of the Liquid Drop Model of nuclear binding energies.

There are a few natural directions to enhance the methodology provided in this work from both computational and theoretical perspectives. First, an *a priori* method to select a sufficient truncation level for vine copulas would be beneficial to avoid the current sequential approach. For example, Brechmann and Joe (2015) discuss the use of fit indices for finding sufficient truncation. Secondly, the theoretical justification for our method would greatly benefit from establishing the link between the ELBO and the l-truncated ELBO which is the ultimate driving force behind the computational efficiency of the VC. Additionally, there are other alternatives to the traditional MCMC than VBI that have shown to be effective in handling massive datasets. The stochastic gradient MCMC (Ma et al., 2015) algorithm, for instance, utilizes similar data subsampling trick as VBI (see Section 2.1 for details) which has been successfully applied in deep learning (Deng et al., 2019) or state space models (Aicher et al., 2019). A similar copula likelihood decomposition to the one proposed in this paper could be used for computer model calibration via stochastic gradient MCMC, however, it would require a non-trivial algorithmic development that is beyond the scope of this work.

## References

- Aicher, C., Y.-A. Ma, N. J. Foti, and E. B. Fox (2019). Stochastic gradient mcmc for state space models. *SIAM Journal on Mathematics of Data Science* 1(3), 555–587.
- Audi, G., A. Wapstra, and C. Thibault (2003). The AME2003 atomic mass evaluation: (ii). tables, graphs and references. *Nuclear Physics A* 729, 337–676.
- Bayarri, M. J., J. O. Berger, R. Paulo, J. Sacks, J. A. Cafeo, J. Cavendish, C.-H. Lin, and J. Tu (2007). A framework for validation of computer models. *Technometrics* 49, 138–154.

- Bedford, T. and R. M. Cooke (2002). Vines—a new graphical model for dependent random variables. *The Annals of Statistics* 30(4), 1031–1068.
- Benzaid, D., S. Bentriddi, A. Kerraci, and N. Amrani (2020). Bethe–Weizsäcker semiempirical mass formula coefficients 2019 update based on AME2016. *Nucl. Sci. Tech.* 31, 9.
- Bertsch, G. F. and D. Bingham (2017). Estimating parameter uncertainty in binding-energy models by the frequency-domain bootstrap. *Physical Review Letters* 119, 252501.
- Bertsch, G. F., B. Sabbey, and M. Uusnäkki (2005, May). Fitting theories of nuclear binding energies. *Phys. Rev. C* 71, 054311.
- Bethe, H. A. and R. F. Bacher (1936, Apr). Nuclear physics a. stationary states of nuclei. *Rev. Mod. Phys.* 8, 82–229.
- Bottou, L., Y. Le Cun, and Y. Bengio (1997). Global training of document processing systems using graph transformer networks. In *Proceedings of Computer Vision and Pattern Recognition (CVPR)*, pp. 489–493. IEEE.
- Brechmann, E. C., C. Czado, and K. Aas (2012). Truncated regular vines in high dimensions with application to financial data. *The Canadian Journal of Statistics* 40(1), 68–85.
- Brechmann, E. C. and H. Joe (2015). Truncation of vine copulas using fit indices. *Journal of Multivariate Analysis* 138, 19–33.
- Casella, G. and C. P. Robert (1996). Rao-blackwellisation of sampling schemes. *Biometrika* 83(1), 81–94.
- Chib, S. and E. Greenberg (1995). Understanding the Metropolis-Hastings algorithm. *The American Statistician* 49, 327–335.
- Cooke, R. and D. Kurowicka (2006). *Uncertainty Analysis With High Dimensional Dependence Modelling*. Wiley.

- Deng, W., X. Zhang, F. Liang, and G. Lin (2019). An adaptive empirical bayesian method for sparse deep learning. In *Advances in Neural Information Processing Systems 32*, pp. 5563–5573. Curran Associates, Inc.
- Dissmann, J., E. Brechmann, C. Czado, and D. Kurowicka (2013). Selecting and estimating regular vine copulae and application to financial returns. *Computational Statistics & Data Analysis* 59, 52–69.
- Dobaczewski, J., W. Nazarewicz, and P.-G. Reinhard (2014, may). Error estimates of theoretical models: a guide. *Journal of Physics G: Nuclear and Particle Physics* 41(7), 074001.
- Duchi, J., E. Hazan, and Y. Singer (2011). Adaptive subgradient methods for online learning and stochastic optimization. *The Journal of Machine Learning Research* 12, 2121–2159.
- Fayans, S. A. (1998). Towards a universal nuclear density functional. *Journal of Experimental and Theoretical Physics Letters* 68(3), 169–174.
- Goldberger, A. (1966). *Econometric theory*. Wiley publications in statistics. J. Wiley.
- Gu, M. and L. Wang (2018). Scaled Gaussian stochastic process for computer model calibration and prediction. *SIAM/ASA Journal on Uncertainty Quantification* 6(4), 1555–1583.
- Higdon, D., J. Gattiker, B. Williams, and M. Rightley (2008). Computer model calibration using high-dimensional output. *Journal of the American Statistical Association* 103, 570–583.
- Higdon, D., M. Kennedy, J. C. Cavendish, J. A. Cafo, and R. D. Ryne (2005). Combining field data and computer simulations for calibration and prediction. *SIAM Journal on Scientific Computing* 26, 448–466.

- Higdon, D., J. D. McDonnell, N. Schunck, J. Sarich, and S. M. Wild (2015). A Bayesian approach for parameter estimation and prediction using a computationally intensive model. *Journal of Physics G: Nuclear and Particle Physics* 42(3), 034009.
- Hoffman, M. and D. Blei (2015, 09–12 May). Stochastic structured variational inference. In *Proceedings of the Eighteenth International Conference on Artificial Intelligence and Statistics*, Volume 38, San Diego, CA, pp. 361–369. PMLR.
- Hoffman, M. D., D. M. Blei, C. Wang, and J. Paisley (2013). Stochastic variational inference. *Journal of Machine Learning Research* 14, 1303–1347.
- Homan, M. D. and A. Gelman (2014). The No-U-Turn Sampler: Adaptively setting path lengths in Hamiltonian Monte Carlo. *Journal of Machine Learning Research* 15, 1351–1381.
- Johnston, J. (1976). *Econometric Methods*. McGraw-Hill.
- Jordan, M. I., Z. Ghahramani, T. S. Jaakkola, and L. K. Saul (1999). An introduction to variational methods for graphical models. *Machine Learning* 37, 183–233.
- Kejzlar, V., L. Neufcourt, W. Nazarewicz, and P.-G. Reinhard (2020). Statistical aspects of nuclear mass models.
- Kennedy, M. C. and A. O’Hagan (2001). Bayesian calibration of computer models. *Journal of the Royal Statistical Society: Series B (Statistical Methodology)* 63, 425–464.
- King, G. B., A. E. Lovell, L. Neufcourt, and F. M. Nunes (2019). Direct comparison between Bayesian and frequentist uncertainty quantification for nuclear reactions. *Physical Review Letters* 122, 232502.
- Kirson, M. W. (2008). Mutual influence of terms in a semi-empirical mass formula. *Nucl. Phys. A* 798(1), 29 – 60.
- Kortelainen, M., T. Lesinski, J. J. Moré, W. Nazarewicz, J. Sarich, N. Schunck, M. V. Stoitsov, and S. M. Wild (2010). Nuclear energy density optimization. *Physical Review C* 82(2), 024313.

- Kortelainen, M., J. McDonnell, W. Nazarewicz, E. Olsen, P.-G. Reinhard, J. Sarich, N. Schunck, S. M. Wild, D. Davesne, J. Erler, and A. Pastore (2014). Nuclear energy density optimization: Shell structure. *Phys. Rev. C* 89, 054314.
- Kortelainen, M., J. McDonnell, W. Nazarewicz, P.-G. Reinhard, J. Sarich, N. Schunck, M. V. Stoitsov, and S. M. Wild (2012). Nuclear energy density optimization: large deformations. *Physical Review C* 85, 024304.
- Krane, K. (1987). *Introductory Nuclear Physics*. Wiley.
- Lawrence, E., K. Heitmann, M. White, D. Higdon, C. Wagner, S. Habib, and B. Williams (2010). The Coyote Universe III: simulation suite and precision emulator for the nonlinear matter power spectrum. *The Astrophysical Journal* 713(2), 1322–1331.
- Ma, Y.-A., T. Chen, and E. Fox (2015). A complete recipe for stochastic gradient mcmc. In C. Cortes, N. D. Lawrence, D. D. Lee, M. Sugiyama, and R. Garnett (Eds.), *Advances in Neural Information Processing Systems 28*, pp. 2917–2925. Curran Associates, Inc.
- McDonnell, J. D., N. Schunck, D. Higdon, J. Sarich, S. M. Wild, and W. Nazarewicz (2015). Uncertainty quantification for nuclear density functional theory and information content of new measurements. *Physical Review Letters* 114(12), 122501.
- Morris, M. D. and T. J. Mitchell (1995). Exploratory designs for computational experiments. *Journal of Statistical Planning and Inference* 43(3), 381 – 402.
- Myers, W. D. and W. J. Swiatecki (1966). Nuclear masses and deformations. *Nucl. Phys.* 81(2), 1 – 60.
- Neiswanger, W., C. Wang, and E. P. Xing (2014). Asymptotically exact, embarrassingly parallel mcmc. In *Proceedings of the Thirtieth Conference on Uncertainty in Artificial Intelligence*, UAI’14, Arlington, VA, pp. 623–632. AUAI Press.
- Peterson, C. and J. R. Anderson (1987). A mean field theory learning algorithm for neural networks. *Complex Systems* 1, 995–1019.

- Plumlee, M. (2017). Bayesian calibration of inexact computer models. *Journal of the American Statistical Association* 112, 1274–1285.
- Plumlee, M. (2019). Computer model calibration with confidence and consistency. *Journal of the Royal Statistical Society: Series B (Statistical Methodology)* 81(3), 519–545.
- Plumlee, M., V. R. Joseph, and H. Yang (2016). Calibrating functional parameters in the ion channel models of cardiac cells. *Journal of the American Statistical Association* 111, 500–509.
- Pollard, D., W. Chang, M. Haran, P. Applegate, and R. DeConto (2016). Large ensemble modeling of the last deglacial retreat of the West Antarctic Ice Sheet: comparison of simple and advanced statistical techniques. *Geoscientific Model Development* 9(5), 1697–1723.
- Quiñonero-Candela, J. and C. E. Rasmussen (2005). A unifying view of sparse approximate Gaussian process regression. *Journal of Machine Learning Research*, 1939–1959.
- Ranganath, R., S. Gerrish, and D. Blei (2014). Black box variational inference. In *Proceedings of the Seventeenth International Conference on Artificial Intelligence and Statistics*, Volume 33 of *Proceedings of Machine Learning Research*, pp. 814–822. PMLR.
- Ranganath, R., D. Tran, and D. M. Blei (2016). Hierarchical variational models. In *Proceedings of the 33rd International Conference on International Conference on Machine Learning – Volume 48*, ICML’16, pp. 2568–2577. JMLR.
- Reinhard, P.-G., M. Bender, W. Nazarewicz, and T. Vertse (2006, Jan). From finite nuclei to the nuclear liquid drop: Leptodermous expansion based on self-consistent mean-field theory. *Phys. Rev. C* 73, 014309.
- Robbins, H. and S. Monro (1951, 09). A stochastic approximation method. *Annals of Mathematical Statistics* 22(3), 400–407.
- Ross, S. M. (2006). *Simulation* (Fourth ed.). Orlando, FL: Academic Press, Inc.

- Ruiz, F. J. R., M. K. Titsias, and D. M. Blei (2016). Overdispersed black-box variational inference. In *Proceedings of the Thirty-Second Conference on Uncertainty in Artificial Intelligence*, UAI16, Arlington, Virginia, USA, pp. 647656. AUAI Press.
- Sexton, D. M. H., J. M. Murphy, M. Collins, and M. J. Webb (2012). Multivariate probabilistic projections using imperfect climate models Part i: outline of methodology. *Climate Dynamics* 38(11), 2513–2542.
- Sklar, A. (1959). Fonctions de répartition à n dimensions et leurs marges. *Publications de l’Institut de Statistique de l’Université de Paris* 8, 229–231.
- Smith, M. S., R. Loaiza-Maya, and D. J. Nott (2020). High-dimensional copula variational approximation through transformation. *Journal of Computational and Graphical Statistics* 0(ja), 1–35.
- Tieleman, T. and G. Hinton (2012). Lecture 6.5—RmsProp: Divide the gradient by a running average of its recent magnitude. COURSERA: Neural Networks for Machine Learning.
- Titsias, M. (2009, 16–18 Apr). Variational learning of inducing variables in sparse Gaussian processes. In *Proceedings of the Twelfth International Conference on Artificial Intelligence and Statistics*, Volume 5, pp. 567–574. PMLR.
- Tran, D., D. M. Blei, and E. M. Airoldi (2015). Copula variational inference. In *Proceedings of the 28th International Conference on Neural Information Processing Systems - Volume 2*, NeurIPS’15, Cambridge, MA, pp. 3564–3572. MIT Press.
- Wang, Y. and D. M. Blei (2018). Frequentist consistency of variational Bayes. *Journal of the American Statistical Association* 0(0), 1–15.
- Weizsäcker, C. F. v. (1935). Zur theorie der kernmassen. *Z. Phys.* 96(7), 431–458.
- Yuan, C. (2016, Mar). Uncertainty decomposition method and its application to the liquid drop model. *Phys. Rev. C* 93, 034310.

Zeiler, M. D. (2012). Adadelta: An adaptive learning rate method. *ArXiv 1212.5701*.

Zhang, L., Z. Jiang, J. Choi, C.-Y. Lim, T. Maiti, and S. Baek (2019). Patient-specific prediction of abdominal aortic aneurysm expansion using Bayesian calibration. *IEEE Journal of Biomedical and Health Informatics*.

## Appendix A Scalable Algorithm with Truncate C-Vine Copulas

Here we present the details of C-vine based version of the Algorithm 1 and the Algorithm 2.

First, we can decompose the log-likelihood  $\log p(\mathbf{d}|\phi)$  using a C-vine as

$$\log p(\mathbf{d}|\phi) = \sum_{j=1}^{n-1} \sum_{i=1}^{n-j} p_{j,j+i}^C(\phi),$$

where  $p_{j,j+i}^C(\phi) = \log c_{j,(j+i);1,\dots,(j-1)} + \frac{1}{n-1} (\log p_j(d_j|\phi) + \log p_{j+i}(d_{j+i}|\phi))$ . This now yields the following expression for the ELBO gradient:

$$\nabla_{\lambda} \mathcal{L}(\lambda) = \sum_{j=1}^{n-1} \sum_{i=1}^{n-j} E_q \left[ \nabla_{\lambda} \log q(\phi|\lambda) (p_{j,j+i}^C(\phi)) \right] - E_q \left[ \nabla_{\lambda} \log q(\phi|\lambda) \log \frac{q(\phi|\lambda)}{p(\phi)} \right].$$

We can, analogously to the D-vine decomposition case, consider the bijection

$$I_C : \left\{ 1, \dots, \frac{n(n-1)}{2} \right\} \rightarrow \left\{ (j, j+i) : i \in \{1, \dots, n-j\} \text{ for } j \in \{1, \dots, n-1\} \right\}$$

and the random variable  $K \sim U(1, \dots, \frac{n(n-1)}{2})$ . We define a noisy estimate of the gradient using C-vine as

$$\tilde{\mathcal{L}}_C(\lambda) := \frac{n(n-1)}{2} E_q \left[ \nabla_{\lambda} \log q(\phi|\lambda) (p_{I_C(K)}^C(\phi)) \right] - E_q \left[ \nabla_{\lambda} \log q(\phi|\lambda) \log \frac{q(\phi|\lambda)}{p(\phi)} \right].$$

Note that this is unbiased (i.e.,  $E(\tilde{\mathcal{L}}_C(\lambda)) = \nabla_\lambda \mathcal{L}(\lambda)$ ) as desired. Again,  $\tilde{\mathcal{L}}_C(\lambda)$  can be relatively costly for large datasets. We therefore decompose the log-likelihood  $\log p(\mathbf{d}|\phi)$  using an  $l$ -truncated C-vine, namely

$$\log p(\mathbf{d}|\phi) = \sum_{j=1}^l \sum_{i=1}^{n-j} p_{j,j+i}^{C_l}(\phi),$$

where

$$\begin{aligned} p_{j,j+i}^{C_l}(\phi) &= \log c_{j,(j+i);1,\dots,(j-1)} + \frac{1}{n-1} \log p_j(d_j|\phi) + \\ &+ \frac{1}{(n-1-l)\mathbb{1}_{j+i \leq l} + l} \log p_{j+i}(d_{j+i}|\phi). \end{aligned}$$

This yields the *l-truncated ELBO* for the  $l$ -truncated C-vine:

$$\mathcal{L}_{C_l}(\lambda) = E_q \left[ \sum_{j=1}^l \sum_{i=1}^{n-j} p_{j,j+i}^{C_l}(\phi) \right] - KL(q(\phi|\lambda) || p(\phi)).$$

Given the bijection

$$I_{C_l} : \left\{ 1, \dots, \frac{l(2n - (l+1))}{2} \right\} \rightarrow \{(j, j+i) : i \in \{1, \dots, n-j\} \text{ for } j \in \{1, \dots, l\}\}$$

and the random variable  $K \sim U(1, \dots, \frac{l(2n-(l+1))}{2})$ , we can get a stochastic estimate of the gradient  $\nabla_\lambda \mathcal{L}_{C_l}(\lambda)$  from

$$\tilde{\mathcal{L}}_{C_l}(\lambda) := \frac{l(2n - (l+1))}{2} E_q \left[ \nabla_\lambda \log q(\phi|\lambda) (p_{I_{C_l}(K)}^{C_l}(\phi)) \right] - E_q \left[ \nabla_\lambda \log q(\phi|\lambda) \log \frac{q(\phi|\lambda)}{p(\phi)} \right],$$

which is unbiased since  $E(\tilde{\mathcal{L}}_{C_l}(\lambda)) = \nabla_\lambda \mathcal{L}_{C_l}(\lambda)$ . See the C-vine based version of Algorithm 1 described below.

---

**Algorithm 3** Variational Calibration with Truncated Vine Copulas (C-vine version)

**Require:** Data  $\mathbf{d}$ , mean and covariance functions for  $\mathcal{GP}$  models in Kennedy-O’Hagan framework, variational family  $q(\phi|\lambda)$ , **truncation level**  $l$

- 1:  $\lambda \leftarrow$  random initial value
  - 2:  $t \leftarrow 1$
  - 3: **repeat**
  - 4:     **for**  $s = 1$  to  $S$  **do** ▷ Random sample  $q$
  - 5:          $\phi[s] \sim q(\phi|\lambda)$
  - 6:     **end for**
  - 7:      $K \leftarrow U(1, \dots, \frac{l(2n-(l+1))}{2})$
  - 8:      $\rho \leftarrow t^{\text{th}}$  value of a Robbins-Monro sequence
  - 9:      $\lambda \leftarrow \lambda + \rho \frac{1}{S} \sum_{s=1}^S \left[ \frac{l(2n-(l+1))}{2} \nabla_{\lambda} \log q(\phi[s]|\lambda) (p_{I_{C_l}(K)}^{C_l}(\phi[s]) - \frac{2}{l(2n-(l+1))} \log \frac{q(\phi[s]|\lambda)}{p(\phi[s])}) \right]$
  - 10:      $t \leftarrow t + 1$
  - 11: **until** change of  $\lambda$  is less than  $\epsilon$
- 

## A.1 Variance Reduction

Let us now consider the MC approximation of the gradient estimator  $\tilde{\mathcal{L}}_{C_l}(\lambda)$ , the  $j^{\text{th}}$  entry of the Rao-Blackwellized estimator is

$$\frac{1}{S} \sum_{s=1}^S \left[ \frac{l(2n-(l+1))}{2} \nabla_{\lambda_j} \log q(\phi_j[s]|\lambda_j) (\tilde{p}_{(j)}(\phi[s]) - \frac{2}{l(2n-(l+1))} \log \frac{q(\phi_j[s]|\lambda_j)}{p(\phi_j[s])}) \right],$$

where  $\tilde{p}_{(j)}(\phi)$  are here the components of  $p_{I_{C_l}(K)}^{C_l}(\phi)$  that include  $\phi_j$ .

We can again use control variates to reduce the variance of MC approximation of the gradient estimator  $\tilde{\mathcal{L}}_{C_l}(\lambda)$ . In particular, we consider the following  $j^{\text{th}}$  entry of the Rao-Blackwellized MC approximation of the gradient estimator  $\tilde{\mathcal{L}}_{C_l}(\lambda)$  with CV

$$\tilde{\mathcal{L}}_{C_l}^{CV(j)}(\lambda) = \frac{1}{S} \sum_{s=1}^S \left[ \frac{l(2n-(l+1))}{2} \nabla_{\lambda_j} \log q(\phi_j[s]|\lambda_j) (\tilde{p}_{(j)}(\phi[s]) - \frac{2(\log \frac{q(\phi_j[s]|\lambda_j)}{p(\phi_j[s])} + \hat{a}_j^C)}{l(2n-(l+1))}) \right],$$

where  $\hat{a}_j^C$  is the estimate of the optimal control variate scalar  $a^*$  based on  $S$  (or fewer) independent draws from variational approximation. Namely

$$\hat{a}_j^C = \frac{\widehat{Cov}_q(\frac{l(2n-(l+1))}{2} \nabla_{\lambda_j} \log q(\phi_j|\lambda_j) (\tilde{p}_{(j)}(\phi) - \frac{2}{l(2n-(l+1))} \log \frac{q(\phi_j|\lambda_j)}{p(\phi_j)}), \nabla_{\lambda_j} \log q(\phi_j|\lambda_j))}{\widehat{Var}_q(\nabla_{\lambda_j} \log q(\phi_j|\lambda_j))}.$$

As in the case of D-vine decomposition, we derive the ultimate version of Algorithm 3 with importance sampling. Again, instead of taking samples from the variational family  $q(\phi|\lambda)$  to approximate the gradient estimates, we will take samples from an overdispersed distribution  $r(\phi|\lambda, \tau)$  in the same family that depends on an additional dispersion parameter  $\tau > 1$ . Combining the ideas of Rao-Blackwellization, CV, and importance sampling, we have the following  $j^{\text{th}}$  entry of the MC approximation of the gradient estimator  $\tilde{\mathcal{L}}_{C_l}(\lambda)$

$$\tilde{\mathcal{L}}_{C_l}^{OCV(j)}(\lambda) = \sum_{s=1}^S \left[ \frac{l(2n - (l + 1))}{2S} \nabla_{\lambda_j} \log q(\phi_j[s]|\lambda_j) (\tilde{p}_{(j)}(\phi[s]) - \frac{2(\log \frac{q(\phi_j[s]|\lambda_j)}{p(\phi_j[s])} + \tilde{a}_j^C)}{l(2n - (l + 1))}) w(\phi_j[s]) \right],$$

where  $\phi[s] \sim r(\phi|\lambda, \tau)$  and  $w(\phi[s]) = q(\phi[s]|\lambda)/r(\phi[s]|\lambda, \tau)$  with

$$\tilde{a}_j^C = \frac{\widehat{Cov}_r\left(\frac{l(2n-(l+1))}{2} \nabla_{\lambda_j} \log q(\phi_j|\lambda_j) (\tilde{p}_{(j)}(\phi) - \frac{2 \log \frac{q(\phi_j|\lambda_j)}{p(\phi_j)}}{l(2n-(l+1))}) w(\phi_j), \nabla_{\lambda_j} \log q(\phi_j|\lambda_j) w(\phi_j)\right)}{\widehat{Var}_r(\nabla_{\lambda_j} \log q(\phi_j|\lambda_j) w(\phi_j))}.$$

The extension of the Algorithm 3 is summarized in the Algorithm 4.

---

**Algorithm 4** Variational Calibration with Truncated Vine Copulas II (C-vine)

---

**Require:** Data  $\mathbf{d}$ , mean and covariance functions for  $\mathcal{GP}$  models in Kennedy-O'Hagan framework, variational family  $q(\phi|\lambda)$ , dispersion parameter  $\tau$ , **truncation level 1**

- 1:  $\lambda \leftarrow$  random initial value
  - 2:  $t \leftarrow 1$
  - 3: **repeat**
  - 4:     **for**  $s = 1$  to  $S$  **do** ▷ Random sample  $q$
  - 5:          $\phi[s] \sim r(\phi|\lambda, \tau)$
  - 6:     **end for**
  - 7:      $K \leftarrow U(1, \dots, \frac{l(2n-(l+1))}{2})$
  - 8:      $\rho \leftarrow t^{\text{th}}$  value of a Robbins-Monro sequence
  - 9:      $\lambda \leftarrow \lambda + \rho \sum_{s=1}^S \left[ \frac{l(2n-(l+1))}{2S} \nabla_{\lambda_j} \log q(\phi_j[s]|\lambda_j) (\tilde{p}_{(j)}(\phi[s]) - \frac{2(\log \frac{q(\phi_j[s]|\lambda_j)}{p(\phi_j[s])} + \tilde{a}_j^C)}{l(2n-(l+1))}) w(\phi_j[s]) \right]$
  - 10:     $t \leftarrow t + 1$
  - 11: **until** change of  $\lambda$  is less than  $\epsilon$
-

## Appendix B Simulation: Memory Profile

Here we present the memory profiles for the MH, the NUTS, and the Algorithm 2 under the simulation scenario studied in Chapter 5. These were recorded during a one hour period of running the algorithms. The MH algorithm and the NUTS were implemented in Python 3.0 using the PyMC3 module version 3.5. The memory profiles were measured using the memory-profiler module version 0.55.0 in Python 3.0. The VC was also implemented in Python 3.0. The code was run on the high performance computing cluster at the Institute for Cyber-Enabled Research at Michigan State University.

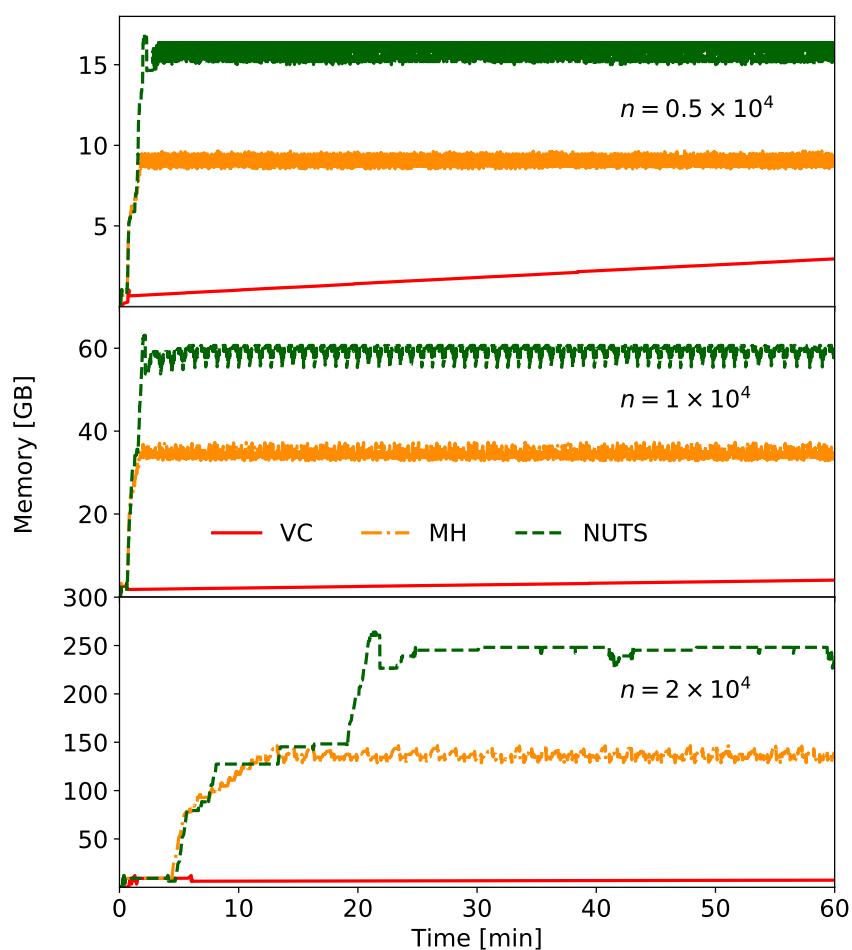


Figure 6: Recorded memory profiles of the Algorithm 2, the MH algorithm, and the NUTS for the duration of 1h under the simulation scenario with  $n = 0.5 \times 10^4$ ,  $n = 1 \times 10^4$ , and  $n = 2 \times 10^4$ .

# Appendix C Application: Liquid Drop Model (LDM)

## C.1 $\mathcal{GP}$ specifications

In the case of the LDM  $E_B(Z, N)$ , we consider the  $\mathcal{GP}$  prior with mean zero and covariance function

$$\eta_E \cdot \exp\left(-\frac{\|Z - Z'\|^2}{2\nu_Z^2} - \frac{\|N - N'\|^2}{2\nu_N^2} - \frac{\|a_{vol} - a'_{vol}\|^2}{2\nu_1^2} - \frac{\|a_{surf} - a'_{surf}\|^2}{2\nu_2^2} - \frac{\|a_{sym} - a'_{sym}\|^2}{2\nu_3^2} - \frac{\|a_C - a'_C\|^2}{2\nu_4^2}\right).$$

Similarly, we consider the  $\mathcal{GP}$  process prior for the systematic discrepancy  $\delta(Z, N)$  with mean zero and covariance function

$$\eta_\delta \cdot \exp\left(-\frac{\|Z - Z'\|^2}{2l_Z^2} - \frac{\|N - N'\|^2}{2l_N^2}\right).$$

## C.2 Experimental design

Kennedy and O'Hagan (2001) recommend to select the calibration inputs for the model runs so that the plausible value  $\theta$  of the true calibration parameter is covered. In this context, we consider the space of calibration parameters to be centered at the values of least squares estimates  $\hat{\theta}_{L_2}$  and broad enough to contain the majority of values provided by the nuclear physics literature (Weizsäcker, 1935; Bethe and Bacher, 1936; Myers and Swiatecki, 1966; Kirson, 2008; Benzaid et al., 2020). Table 4 gives the lower and upper bounds for the parameter space so that Lower bound =  $\hat{\theta}_{L_2} - 15 \times SE(\hat{\theta}_{L_2})$  and Upper bound =  $\hat{\theta}_{L_2} + 15 \times SE(\hat{\theta}_{L_2})$ . Here  $SE(\hat{\theta}_{L_2})$  is given by the standard linear regression theory.

Table 4: The space of calibration parameters used for generating the outputs of semi-empirical mass formula (31).

Parameter	Lower bound	Upper bound
$a_{vol}$	15.008	15.829
$a_{surf}$	15.628	18.193
$a_{sym}$	21.435	23.505
$a_C$	0.665	0.72

### C.3 Prior distributions

First, we consider the independent Gaussian distributions centered at the LS estimates  $\hat{\theta}_{L_2}$  (in Table 3) with standard deviations  $7.5 \times SE(\hat{\theta}_{L_2})$  so that the calibration parameters used for generating the model runs are covered roughly within two standard deviations of the priors. Namely,

$$a_{vol} \sim N(15.42, 0.203),$$

$$a_{surf} \sim N(16.91, 0.645),$$

$$a_{sym} \sim N(22.47, 0.525),$$

$$a_C \sim N(0.69, 0.015).$$

The prior distributions for hyperparameters of the  $GP$ 's were selected as  $Gamma(\alpha, \beta)$  with the scale parameter  $\alpha$  and rate parameter  $\beta$ , so that they represent a vague knowledge about the scale of these parameters given by the literature on nuclear mass models (Weizsäcker, 1935; Bethe and Bacher, 1936; Myers and Swiatecki, 1966; Fayans, 1998; Kirson, 2008; McDonnell et al., 2015; Kortelainen et al., 2010, 2012, 2014; Benzaid et al., 2020; Kejzlar et al., 2020).

The error scale  $\sigma$  is in the majority of nuclear applications within units of MeV, therefore we set

$$\sigma \sim Gamma(2, 1)$$

with the scale of systematic error being

$$\eta_\delta \sim \text{Gamma}(10, 1)$$

to allow for this quantity to range between units and tens of MeV. It is also reasonable to assume that the mass of a given nucleus is correlated mostly with the its neighbours on the nuclear chart. We express this notion through reasonably wide prior distributions

$$\begin{aligned} l_Z &\sim \text{Gamma}(10, 1), \\ l_N &\sim \text{Gamma}(10, 1), \\ \nu_Z &\sim \text{Gamma}(10, 1), \\ \nu_N &\sim \text{Gamma}(10, 1), \\ \nu_i &\sim \text{Gamma}(10, 1), \quad i = 1, 2, 3, 4. \end{aligned}$$

Finally, the majority of the masses in the training dataset of 2000 experimental binding energies fall into the range of [1000, 2000] MeV (1165 precisely). We consider the following prior distribution for the parameter  $\eta_f$  to reflect on the scale of the experimental binding energies:

$$\eta_f \sim \text{Gamma}(110, 10).$$